

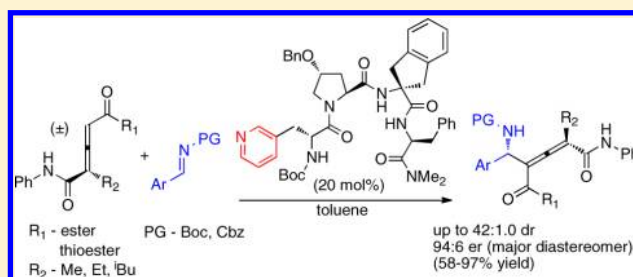
Diastereo- and Enantioselective Addition of Anilide-Functionalized Allenates to *N*-Acylimines Catalyzed by a Pyridylalanine-Based Peptide

Curren T. Mbofana and Scott J. Miller*

Department of Chemistry, Yale University, P.O. Box 208107, New Haven, Connecticut 06520-8107, United States

S Supporting Information

ABSTRACT: A selective peptide-catalyzed addition of allenic esters to *N*-acylimines is reported. Tetrasubstituted allenates were achieved with up to 42:1 diastereomeric ratio and 94:6 enantiomeric ratio (up to 99:1 er after recrystallization of the major diastereomer). An exploration of the role of individual amino acids within the peptide was undertaken. The scope of the reaction was explored and revealed heightened reactivity with thioester-containing allenates. A mechanistic framework that may account for the observed reactivity is also described.



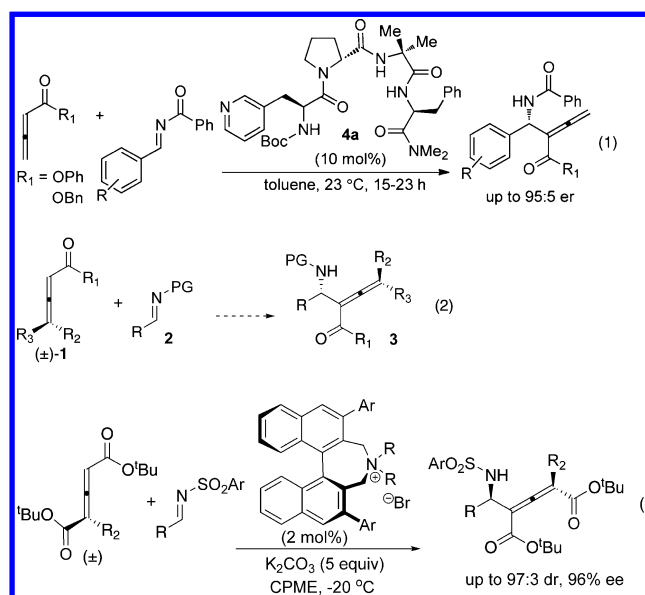
INTRODUCTION

The allene moiety is an important functional group in organic synthesis and medicine. It is found in a number of natural products and pharmaceutical compounds.^{1,2} Moreover, the unique reactivity of allenes renders them versatile intermediates in organic synthesis.^{3–10} Numerous methods for stereoselective synthesis of di- and trisubstituted allenes have been developed.^{11,12} However, access to chiral tetrasubstituted allenes remains a challenge, and limited examples exist.^{13–16}

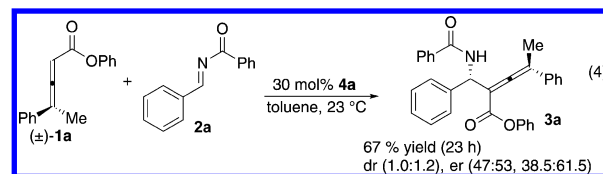
Our laboratory has been interested in the use of nitrogen-based catalysts for additions of nucleophiles,^{17–19} including allenate esters^{20,21} to various electrophiles such as α,β -unsaturated carbonyl compounds and *N*-acylimines. In 2009, our laboratory disclosed an enantioselective coupling reaction of allenic esters to imines using a pyridylalanine (Pal)-based peptide catalyst (eq 1).¹⁶ As a nontrivial extension to this work, we envisioned that the coupling of a racemic allene (1) to an *N*-acylimine (2) would deliver a tetrasubstituted allenate (3). Such products (3) possess two elements of stereochemistry, a stereogenic center and an axis of chirality (eq 2). Thus, catalytic reactions of this type would allow an examination of the interplay of the stereogenic center with the axis of chirality during a complex reaction mechanism. We hoped to control both diastereo- and enantioselectivity using peptide-based catalysts. To our knowledge, the only example of a similar transformation is a report published recently by Maruoka and co-workers of a diastereo- and enantioselective addition of di-*tert*-butyl allenic esters to sulfonyl imines, using phase-transfer catalysis (eq 3).²²

RESULTS AND DISCUSSION

Preliminary studies in our laboratory focused on the γ,γ -substituted allene substrate **1a**, employing conditions that had been previously established for the unsubstituted addition



reaction (eq 4).²³ Notably, the reaction proceeded with acceptable conversion, despite the increased steric demands

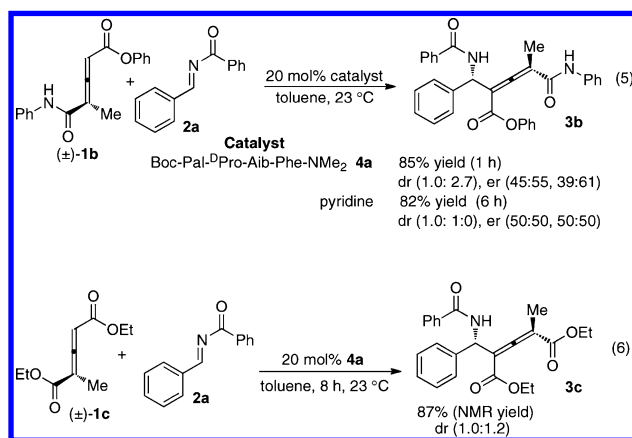


Received: December 20, 2013

Published: February 14, 2014

of the γ,γ -disubstitution in the substrate. With 30 mol% of catalyst **4a**, the reaction proceeded smoothly to deliver **3a** in 67% isolated yield as a combined mixture of stereoisomers within 23 h. However the diastereomeric ratio (dr) was poor (1.0:1.2), and the dominant diastereomer exhibited modest, yet appreciable, enantiomeric ratio (er) of 38.5:61.5. Changing reaction variables such as solvent, temperature, and incorporation of Lewis acidic additives did not improve dr.²⁴

We hypothesized that employing a substrate that contained an additional hydrogen bond donor or acceptor might perturb diastereoselectivity. Our analysis was superficial but hinged on the idea that peptide catalyst–substrate interactions involving hydrogen bonds are supported by extensive experimental evidence.^{25,26} Switching to the anilide allenic ester **1b** provided an observation consistent with this hypothesis (eq 5). With 20



mol% of catalyst **4a** the reaction delivered product **3b** in 85% isolated yield in just 1 h and an improved dr of 1.0:2.7 while maintaining an er of 39:61 for the major diastereomer. Use of pyridine as the catalyst showed no diastereoselectivity, and the reaction was considerably slower, requiring 6 h to reach a comparable level of conversion. Moreover, replacing the anilide group with an ester group eroded dr to 1.0:1.2 (eq 6). These observations support the importance of the anilide group, possibly as a hydrogen bond participant.

Encouraged by these results, we performed a catalyst screen to investigate the optimum diastereomer for the peptide catalyst. In an arbitrary manner, we initially elected to maintain the identity of the amino acids to allow a direct assessment of stereochemical issues. The results are shown in Table 1. The most notable change resulted from switching the $i + 3$ residue from Phe to D-Phe (Table 1, entry 2, peptide **4b**) leading to a slight increase in dr to 1.0:3.0 and an improved er of 22:78 for the major diastereomer. The minor diastereomer er was marginally decreased. However switching the $i + 1$ residue from D-Pro to Pro led to diminished dr (1.0:1.1) regardless of which Phe enantiomer was at the $i + 3$ position (Table 1, entries 3 and 4). Further optimization of peptide **4b** by switching the C-terminal functional group to *N,N*-dimethylamide slightly improved the dr to 1.0:3.4. The er of the major diastereomer remained unchanged, while the er of the minor diastereomer slightly increased to 39:61 (Table 1, entry 5, peptide **4e**).

Having identified a more robust peptide catalyst **4e**, we set out to investigate the effect of the allenic ester group. Replacement of the phenyl ester (Table 2, entry 1) with a benzyl ester resulted in an increase in dr to 1.0:4.3 (Table 2, entry 2). In addition, the reaction required an extended

Table 1. Diastereomeric Peptide Catalyst Screen^a

entry	catalyst	$i + 1$	$i + 3$	X	yield ^b (%)	dr ^c	er (min, maj) ^d
1	4a	D-Pro	Phe	NMe ₂	85	1.0:2.7	45:55, 39:61
2	4b	D-Pro	D-Phe	OMe	80	1.0:3.0	46:54, 22:78
3	4c	Pro	Phe	OMe	85	1.0:1.1	ND
4	4d	Pro	D-Phe	OMe	76	1.0:1.1	ND
5	4e	D-Pro	D-Phe	NMe ₂	71	1.0:3.4	39:61, 22:78

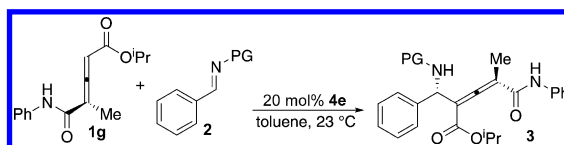
^aReactions were run with 1.2 equiv of allenic ester. ^bTotal yield of both diastereomers determined by ¹H NMR using an internal standard. ^cDetermined by ¹H NMR. ^dDetermined using HPLC with chiral stationary phase. ND: Not determined.

reaction time of 3 h. For aliphatic groups (Table 2, entries 3–5) the bulkier isopropyl group gave the highest dr of 1.0:6.2. Unfortunately, the *tert*-butyl allenic ester could not be successfully synthesized. In addition, more electron-rich ester groups required longer reaction times. For example, with isopropyl allenic ester the reaction required 8 h to reach completion (Table 2, entry 5). It is worth noting that although significant perturbations were observed in terms of the dr and reaction times, the identity of the ester moiety had only a small effect on the observed er of the major diastereomer.

The effect of the reaction solvent was also investigated. Generally, aromatic solvents performed similarly to toluene in both yield and selectivity (Table 2, entries 6–8), with the exception of electron-deficient hexafluorobenzene, in which a decreased dr of 1.0:5.0 and only 48% yield were observed (Table 2, entry 8). CHCl₃ provided **3g** in 1.0:4.4 dr, while DCM and THF revealed lower dr's of 1.0:2.5 and 1.0:2.2 dr, respectively (Table 2, entries 9–11). In addition, lower yields were observed in these solvents, ranging from 55% to 73% in 8 h. Hence, toluene was retained as the solvent of choice.

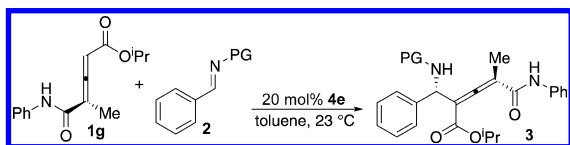
Next, we set out to investigate the impact of the imine-protecting group in Table 3. *N*-Diphenylphosphinoylimine gave no reaction after 24 h (Table 3, entry 1). Yet, *N*-carboxyethylimine gave an improved dr of 1.0:9.3 but with a slightly diminished er of 25:75 (Table 3, entry 2). Switching to the bulkier Boc group resulted in a further increase in dr to 1.0:12, although again a lower er was observed (27:73; Table 3, entry 3). Cyclohexylcarbonyl imine **2e** reactivity was similar to the Boc group (Table 3, entry 4). We chose to proceed with Boc imine due to ease of synthesis.

Encouraged by these results, we examined additional peptide sequences, and the results are shown in Table 4. For this peptide series, the relative stereochemistry in the sequence was kept constant, while the identities of several amino acid side chains were altered. For the $i + 3$ position, switching Aib (2-aminoisobutyric acid) with Acp (1-aminocyclopropane-1-carboxylic acid) gave a minute change in selectivity (Table 4, entries 1 and 2). However, Aic (2-aminoindane-2-carboxylic acid) replacement in peptide **4h** resulted in significant er increase to 20:80 (Table 4, entry 3). Owing to the ready availability of *trans*-4-hydroxy-L-proline, a pseudoenantiomeric

Table 2. Variation to the Allenic Ester Group and Solvent Screen^a

entry	R ₁	solvent	rxn time (h)	Prd	yield (%) ^b	dr ^c	er (maj) ^d
1	OPh, 1b	toluene	1	3b	71	1.0:3.4	22:78
2	OBn, 1d	toluene	3	3d	>95	1.0:4.3	22:78
3	OMe, 1e	toluene	8	3e	>95	1.0:5.0	21:79
4	OEt, 1f	toluene	8	3f	>95	1.0:5.0	21:79
5	O ⁱ Pr, 1g	toluene	8	3g	93	1.0:6.2	22:78
6	O ⁱ Pr, 1g	benzene	8	3g	92	1.0:6.1	21:79
7	O ⁱ Pr, 1g	mesitylene	8	3g	94	1.0:6.2	26:74
8	O ⁱ Pr, 1g	hexafluorobenzene	8	3g	48	1.0:5.0	ND
9	O ⁱ Pr, 1g	chloroform	8	3g	55	1.0:4.4	34:66
10	O ⁱ Pr, 1g	dichloromethane	8	3g	73	1.0:2.5	ND
11	O ⁱ Pr, 1g	tetrahydrofuran	8	3g	60	1.0:2.2	ND

^aReactions were run with 1.2 equiv of imine. ^bTotal yield of both diastereomers determined by ¹H NMR using an internal standard. ^cDetermined by ¹H NMR. ^dDetermined using HPLC with chiral stationary phase. ND: Not determined.

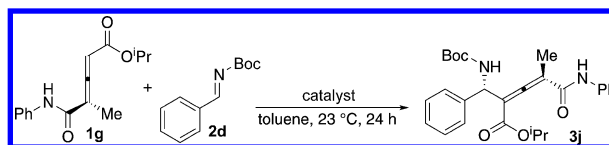
Table 3. Variation to the Imine Protecting Group^a

entry	PG	rxn time (h)	prd	yield ^b (%)	dr ^c	er (maj) ^c
1	POPh ₂ , 2b	24	3h	NR	—:—	—:—
2	CO ₂ Et, 2c	10	3i	72	1.0:9.3	25:75
3	CO ₂ ^t Bu, 2d	8	3j	78	1.0:12	27:73
4	C(O)cyclohexyl, 2e	24	3k	>95	1.0:12 ^d	28:72

^aReactions were run with 1.2 equiv of imine. ^bTotal yield of both diastereomers determined by ¹H NMR using an internal standard. ^cDetermined using HPLC with chiral stationary phase. ^dDetermined by ¹H NMR. NR: no reaction.

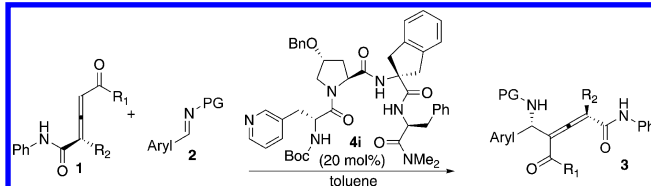
peptide of **4h**, peptide **4i**, was synthesized. The result was a remarkable improvement in both dr (1:17) and er (89:11) (Table 4, entry 4). It is worth noting that although the preferred enantiomer was of course reversed, the major diastereomer remained the same. Further changes to **4i** in the *i* + 3 position by replacing phenylalanine with phenylglycine or *O*-benzyltyrosine were not beneficial (Table 4, entries 5 and 6). Elongating the catalyst sequence to a pentamer did not improve selectivity either (Table 4, entries 7 and 8). Hence, **4i** was identified as the lead peptide catalyst.

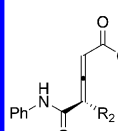
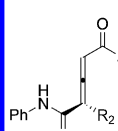
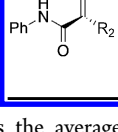
A screen of catalyst loading revealed that conversion decreased with lower amounts of catalyst. The addition reaction was carried out with 10, 5, and 2 mol % of peptide **4i**, resulting in 79, 62, and 29% of product, respectively, within 24 h (Table 4, entries 9–11). Nonetheless, higher product yield was achieved with longer reaction times; 88% yield was achieved with 10 mol % of catalyst after 36 h (Table 4, entry 9), while 5 mol % of catalyst gave 79% yield in 48 h (Table 4, entry 10). Peptide catalyst **4i** was used to examine the substrate scope

Table 4. Peptide Catalyst Reoptimization and Catalyst Loading Screen^a

entry	catalyst	catalyst (mol %)	yield (%) ^b	dr ^c	er (maj) ^c
1	Boc-Pal-D-Pro-Aib-D-Phe-NMe ₂ , 4f	20	78	1.0:12	27:73
2	Boc-Pal-D-Pro-Acp-D-Phe-NMe ₂ , 4g	20	75	1.0:11	26:74
3	Boc-Pal-D-Pro-Aic-D-Phe-NMe ₂ , 4h	20	81	1.0:13	20:80
4	Boc-D-Pal-Hyp(OBn)-Aic-Phe-NMe ₂ , 4i	20	92	1.0:17	89:11
5	Boc-D-Pal-Hyp(OBn)-Aic-Phg-NMe ₂ , 4j	20	87	1.0:12	85:15
6	Boc-D-Pal-Hyp(OBn)-Aic-Tyr(OBn)-NMe ₂ , 4k	20	>95	1.0:15	87:13
7	Boc-D-Pal-Hyp(OBn)-Aic-Phe-D-Phe-NMe ₂ , 4l	20	81	1.0:11	86:14
8	Boc-D-Pal-Hyp(OBn)-Aic-Phe-Phe-NMe ₂ , 4m	20	79	1.0:12	83:17
9	Boc-D-Pal-Hyp(OBn)-Aic-Phe-NMe ₂ , 4i	10	79 (88) ^d	1.0:16	88:12
10	Boc-D-Pal-Hyp(OBn)-Aic-Phe-NMe ₂ , 4i	5	62 (79) ^e	1.0:18	88:12
11	Boc-D-Pal-Hyp(OBn)-Aic-Phe-NMe ₂ , 4i	2	29	1.0:15	89:11

^aReactions were run with 1.2 equiv of imine. ^bTotal yield of both diastereomers determined by ¹H NMR using an internal standard. ^cDetermined using HPLC with chiral stationary phase. ^dYield after 36 h. ^eYield after 48 h.

Table 5. Substrate Scope for Allenic Esters **1** and *N*-Acylimines **2** To Give Addition Products **3** Using Peptide Catalyst **4i**^a


allenic ester	entry	imine (PG Aryl)	reaction time	temp	prd	yield (%) ^b	dr ^d	er (major) ^d
 R ₂ = Me 1g	1	Boc Ph, 2d	24 h	23 °C	3j	91	1.0:16	88:12
	2	Boc <i>p</i> -OMe-Ph, 2f	24 h	23 °C	3l	85	1.0:17	87:13
	3	Boc <i>p</i> -Br-Ph, 2g	24 h	23 °C	3m	95	1.0:10	85.5:14.5
						44		98:2 ^e
	4	Boc <i>p</i> -NO ₂ -Ph, 2h	6 h	23 °C	3n	97	1.0:4.3	79.5:20.5
						ND		99:1 ^e
 R ₂ = Et, 1h	5	Boc 2-thienyl, 2i	12 h	23 °C	3o	94	1.0:8.7	88:12
	6	Cbz Ph, 2j	18 h	23 °C	3p	93	1.0:10	89:11
	7	Boc Ph, 2d	120 h	23 °C	3q	70	1.0:11	71.5:28.5
	8	Cbz Ph, 2j	15 h	-20 °C	3r	81	1.0:25	94:6
	9	Cbz <i>p</i> -Me-Ph, 2k	15 h	-20 °C	3s	78 ^c	1.0:24	93:7
	10	Cbz <i>o</i> -Me-Ph, 2l	15 h	-20 °C	3t	90 ^c	1.0:42	94:6
	11	Cbz <i>p</i> -CF ₃ -Ph, 2m	15 h	-20 °C	3u	95 ^c	1.0:18	88:12
 R ₂ = Et, 1j	12	Cbz Ph, 2j	72 h	-20 °C	3v	80	1.0:13	87.5:12.5
	13	Cbz Ph, 2j	96 h	23 °C	3w	58	1.0:5.8	75.5:24.5

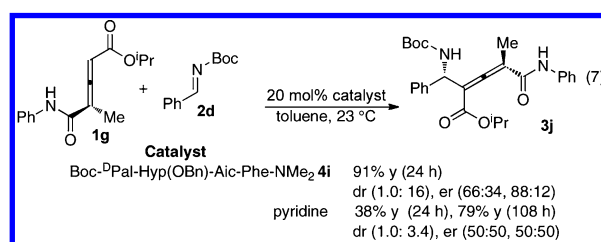
^aAll data is the average of two experiments run using 1.2 equiv of imine. ^bTotal isolated yield of both diastereomers. ^cTotal yield of both diastereomers determined by ¹H NMR using an internal standard. ^dDetermined using HPLC with chiral stationary phase. ^eAfter recrystallization of major diastereomer. ND: not determined.

while maintaining a 20 mol % catalyst loading due to shorter reaction times.

As outlined in Table 5, the optimized catalytic system was successfully applied to a broad substrate scope in good yields and selectivity. Addition product **3j** was obtained in 91% isolated yield, 1.0:16 dr, and 88:12 er after 24 h (Table 5, entry 1). As evidenced by product **3l** (Table 5, entry 2), electron-rich substitution on the imine aryl ring had a negligible effect on dr and er. However, electron-deficient substitution diminished selectivity. *p*-Bromo product **3m** had a dr of 1.0:10 and 85.5:14.5 er (Table 5, entry 3). Furthermore, the pure major diastereomer was enantioenriched by recrystallization of the racemate from toluene, leaving enantioenriched **3m** (98:2 er) in the mother liquor with 44% recovery (based on the sample subjected to recrystallization). The electronic effect was even more pronounced for the *p*-nitro product **3n**, with a poor dr (1.0:4.3) and er (20.5:79.5). In addition, there was significant rate acceleration, and the reaction was complete in 6 h (Table 5, entry 4). Similarly, the **3n** major diastereomer was enantioenriched to 99:1 er by recrystallization from ethyl acetate. Once again, the racemate crystallized while the mother liquor was enriched. The addition reaction tolerated the 2-thienyl heterocycle giving a decent dr of 1.0:8.7 and a comparable er of 88:12 (Table 5, entry 5). Replacement of the Boc group with the Cbz group gave a marginally improved er of 89:11, though the dr was greatly diminished to 1.0:10 (Table 5, entry 6). In addition, this reaction was slightly faster, reaching completion in 18 h. It emerged that the reaction was sensitive to steric bulk on the allenic ester substrate. The reaction with ethyl substrate **1h** required 120 h to deliver product **3q** in 70% isolated yield with a moderate selectivity of 1.0:11 dr and 71.5:28.5 er (Table 5, entry 7).

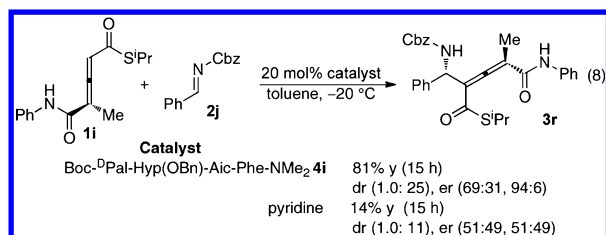
Further substrate and reaction condition optimization revealed that allenic thioester substrates at low temperature have superior reactivity. Allenic thioester **1i** and Cbz-imine **2j** at -20 °C reacted to give product **3r** in excellent selectivity (Table 5, entry 8; 1:25 dr and 94:6 er). As observed with the allenic oxo-ester reactions, the electron-rich *p*-methyl substitution in **2k** had little effect in selectivity (Table 5, entry 9). *o*-Methyl product **3t** (Table 5, entry 10) was obtained in excellent dr of 1.0:42 while maintaining a 94:6 er. The electron-deficient *p*-CF₃ product **3u** gave slightly diminished selectivity (Table 5, entry 11). Also in line with earlier observations, sterically bulky substituents significantly slowed the reaction and resulted in decreased selectivity. Product **3v** was obtained after 72 h in a diminished 1.0:13 dr and 87.5:12.5 er (Table 5, entry 12). This effect was even more pronounced for the bulkier isobutyl allenic ester **1k**, which required 96 h at 23 °C to deliver 58% isolated yield of product **3w** in a poor 1.0:5.8 dr and 75.5:24.5 er (Table 5, entry 13). Nonetheless, it is quite interesting that even with significantly extended reaction time the reaction still proceeded cleanly to the addition product.

A catalyst comparison study was undertaken to better understand the reactivity of allenic oxo- and thioesters under pyridine and peptide catalysis (eq 7). With peptide catalyst **4i**,



the reaction proceeded to allow isolation of the product in 91% yield and 1.0:16 dr in 24 h at 23 °C with 66:34 and 88:12 er for the minor and major diastereomers, respectively. On the other hand, with pyridine as catalyst, only 38% yield was observed within the same time frame, with a dr of 1.0:3.4 and racemic products. To reach a comparable yield (79%), the pyridine-catalyzed reaction required 108 h of reaction time.

Likewise for the thioester reaction (eq 8), at –20 °C the peptide-catalyzed reaction gave a higher yield of 81% within 15



h and a 1.0:25 dr with 69:31 and 94:6 er for the minor and major diastereomers, respectively. Yet, the pyridine-catalyzed reaction gave only 14% yield in 15 h; perhaps surprisingly, in this case a high dr of 1.0:11 was noted. The high dr could be the result of an apparent hydrogen bond present in the crystal structure of the major diastereomer. Figure 1 shows the X-ray

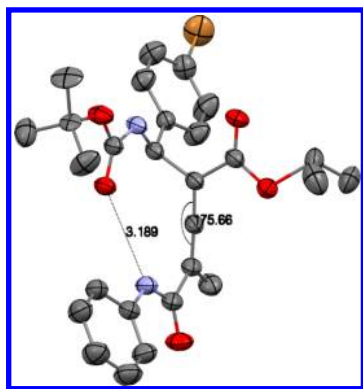
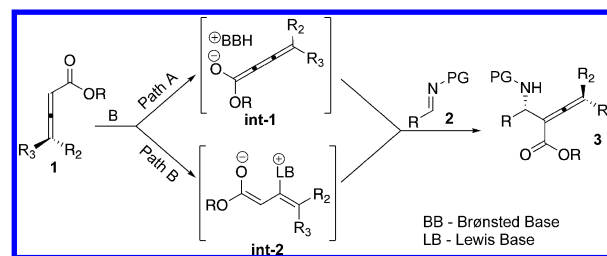


Figure 1. ORTEP representation of the X-ray crystal structure of the major diastereomer racemate of **3m** showing the relative stereochemistry of an arbitrary enantiomer. Ellipsoids drawn at 30% probability level.

structure of addition product **3m**. In Figure 1, the carbamate carbonyl oxygen and anilide nitrogen are 3.19 Å apart, possibly indicative of a hydrogen bond that may develop in the transition state. If the major diastereomer exhibiting this favorable interaction is preferred even with an unfunctionalized, nonpeptidic catalyst, it may be that the peptides amplify the dr in an as yet unknown manner. We note that the X-ray structure shown in Figure 1 was derived from crystals obtained from racemic material of the major diastereomer. Thus, the absolute configuration of our products remains unassigned and is only drawn in analogy to that observed in our earlier study.²³

We then turned our attention to mechanistic issues, ultimately in pursuit of an understanding of both bond-forming steps and the mode of stereoinduction by the chiral catalyst. We consider two possible mechanistic pathways for the formation of addition products under basic conditions as shown in Scheme 1. In one case, proposed by Maruoka and co-workers, a cumulenolate intermediate of type **int-1**, resulting from α -deprotonation of the allenic ester undergoes addition to

Scheme 1. Possible Mechanistic Pathways to Addition Product **3** under Basic Conditions



give product **3** (Scheme 1, path A).²² Under the strongly basic conditions of the Maruoka study (5 equiv of K₂CO₃ or 50% KOH_{aq}), this pathway seems plausible. On the other hand, for nitrogen-containing bases an alternative pathway involving nucleophilic catalysis in analogy to the Morita–Baylis–Hillman-type mechanism could be considered.^{27–33} Nucleophilic addition to the allenic β -carbon would result in zwitterionic intermediate **int-2**. Addition of this species to the imine would ultimately lead to product **3** (Scheme 1, path B). It seems plausible that this alternative mechanism might operate in the presence of weaker bases that are strongly nucleophilic, as we have previously considered.³⁴

To further probe the deprotonation mechanism (path A) versus the addition mechanism (path B), we conducted several experiments, yielding results consistent with our assertions for the peptide-catalyzed pathway. Deuterium-exchange studies were carried out with allenic diester **1c** under various basic conditions with D₂O or MeOD-*d*₄ as the source of the deuterium electrophile, using ¹H NMR. Notably, under Maruoka's phase-transfer conditions,²² H/D exchange occurred rapidly revealing 100% deuterium incorporation with K₂CO₃ (Figure 2a, blue line) and 85% with KOH (Figure 2b, red line)

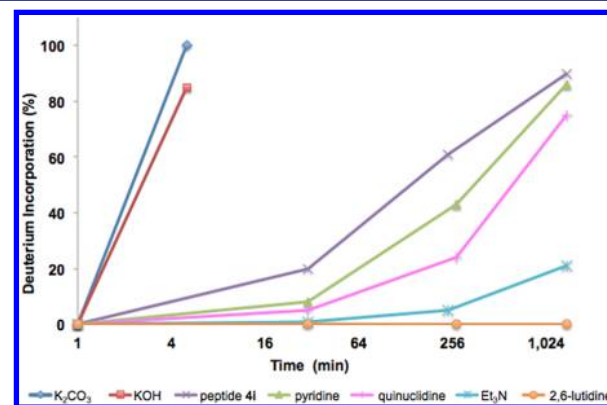
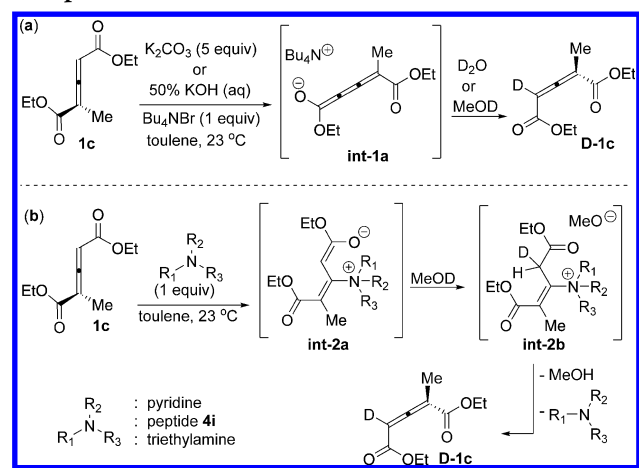


Figure 2. Plot of % deuterium incorporation of **1c** to **D-1c** against time for the following reaction conditions in toluene-*d*₈: (a) K₂CO₃ (5 equiv), Bu₄NBr (1 equiv), MeOD-*d*₄; (b) 50% KOH/D₂O, Bu₄NBr (1 equiv); (c) peptide **4i** (1 equiv), MeOD-*d*₄; (d) pyridine (1 equiv), MeOD-*d*₄; (e) quinuclidine (1 equiv), MeOD-*d*₄; (f) Et₃N (1 equiv), MeOD-*d*₄; (g) 2,6-lutidine (1 equiv), MeOD-*d*₄.

within 5 min. These results are consistent with the role of the proposed cumulenolate intermediate **int-1a** en route to **D-1c** as shown in Scheme 2a. However, H/D exchange was much slower for peptide catalyst **4i** (Figure 2c, purple line) and pyridine (Figure 2d, green line), both of which are relatively weaker bases, reaching 90% and 86%, respectively, over 23 h. Yet, other nitrogen bases that are of various orders of

Scheme 2. Pathways to Account for the Observed Deuterium Incorporation Pattern



magnitude *stronger* as bases than pyridine induced slower H/D exchange than that of the pyridyl catalysts. Quinuclidine (Figure 2e, pink line) gave 75%, and Et₃N (Figure 2f, aqua line) gave only 21%, while no deuterium incorporation was observed for 2,6-lutidine (Figure 2g, orange line) within 23 h. Correlation of kinetic rate data to thermodynamic basicity data must be done cautiously.^{35–37} Nonetheless, the lack of a rigorous pK_a correlation in the deuteration data of Figure 2 supports a possible difference in mechanism. Notably, in scales of nucleophilicity that take into account both electronic and steric effects, pyridine emerges a better nucleophile than does 2,6-lutidine³⁸ or Et₃N.^{39,40} Other scales reveal a different hierarchy.⁴¹ Nevertheless, it is plausible that the deuteration rates are consistent with a possible change in mechanism, from general base catalysis to nucleophilic catalysis,⁴² as one switches from phase transfer to pyridine-induced catalysis.

It is perhaps not surprising that the two mechanisms might induce H/D exchange at very different rates. Scheme 2b shows a pathway that could account for H/D exchange under nucleophilic catalysis. Zwitterionic enolate **int-2a** may react with a deuteron to result in intermediate **int-2b** and, upon subsequent deprotonation and catalyst elimination, yield **D-1c**. Given the highly substituted nature of the allenic substrates, it is conceivable that addition of the relatively bulky Et₃N or quinuclidine or sterically hindered 2,6-lutidine would lead to undesirable steric interactions, ultimately slowing down the reaction significantly when compared to pyridine-based catalysts.

To further interrogate the peptide-catalyzed transformation, we carried out kinetic studies employing allenolate **1g**, imine **2d**, and peptide catalyst **4i** (i.e., eq 7; see the Supporting Information for experimental details and rate plots). The reaction was found to be first order in allenolate and peptide (Table 6), but the rate dependence on imine was very small at synthetically relevant concentrations and could be interpreted as close to zero order and consistent with imine saturation (see Supporting Information).⁴³ These results parallel the experimental observations with the simple allenates studied previously³⁴ and imply that the rate-determining step could involve allenolate and peptide only. Hence, the formation of intermediate **int-1** or **int-2** (Scheme 1) is plausibly the rate-limiting step.

Perhaps more revealing, however, are kinetic isotope effects (KIE) studies that support path B for the peptide-catalyzed

Table 6. Kinetic Order of Allenolate and Peptide for the Transformation in eq 7^a

compd	kinetic order	linear fit correlation constant	power fit exponent (correlation constant)
1g	1	0.999	1.00 (0.999)
4i	1	0.993	0.966 (0.987)

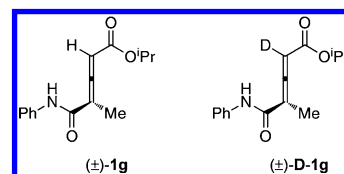
^aSee Supporting Information for reaction details and rate plots at the various concentrations. Linear and power fits and correlation constants were determined using the trendline feature in Microsoft Excel.

Table 7. Kinetic Isotope Effect for Allenolate α -Proton for the Transformation in eq 7^a

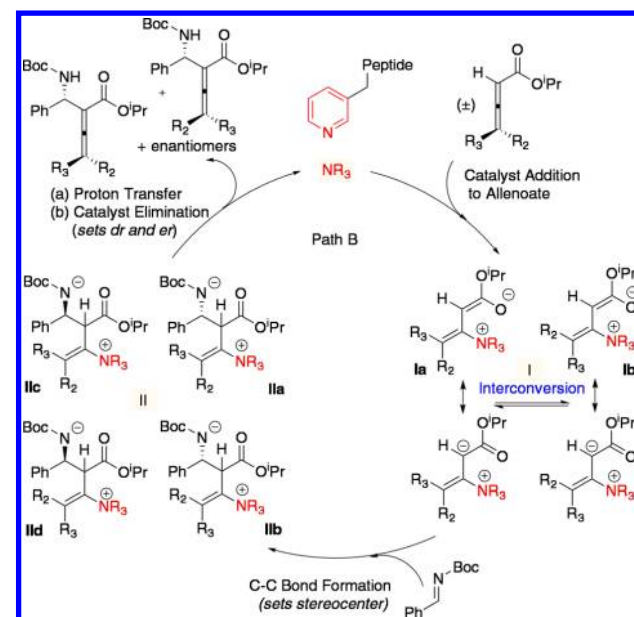
parameter	average ^b
k_H (min ⁻¹)	0.424
k_D (min ⁻¹)	0.415
k_H/k_D	1.02

^aSee the Supporting Information for reaction rate plots. ^bAverage of three runs.

reaction. When the rates exhibited by **1g** (α -H) and **D-1g** (α -D) were compared, the kinetic isotope effect, k_H/k_D , was found to be 1.02 (Table 7). If deprotonation to form **int-1** were the rate-determining step, a significant primary KIE would be observed. Taken together, our kinetic studies are consistent with an addition mechanism (path B) for the peptide-catalyzed reaction.



Scheme 3 shows a speculative, more detailed mechanistic hypothesis for the pyridyl-catalyzed addition transformation

Scheme 3. Mechanistic Hypothesis for Peptide-Catalyzed Addition Reaction^a

^aR₂ = methyl, R₃ = anilide.

involving nucleophilic catalysis. In this mechanism, peptide catalyst **4i** engages in nucleophilic attack on the allenic β -carbon to form a zwitterionic intermediate **I**, which may exist as a variety of isomers, (e.g., **Ia** and **Ib**). However, the delocalized nature of the zwitterion suggests that interconversion among these isomers is possible and possibly subject to catalyst control. Notably, at this stage in the reaction coordinate, any conformational bias resulting from the axial chirality of the racemic allenic starting material enantiomers is likely lost. Next, intermediate **I** attacks the *N*-acylimine to form the C–C bond in intermediate **II**, an event that also sets the stereogenic *N*-bearing carbon center. At least four isomers involving the newly formed stereocenter and the double bond configuration may be considered (**IIa–d**), and again, the catalyst would still exert conformational bias on these isomers. Subsequent α -proton transfer and catalyst elimination would give the addition products, and this final event would define the axis of chirality. Thus, it is possible that the catalyst addition step is rate-determining, but not the stereochemistry-determining step.³⁴

Another critical aspect of our study concerning stereoinduction concerns the actual three-dimensional architecture of the catalyst. Data obtained from ^1H NMR experiments (^1H – ^1H NOESY) (Figure 3a) are consistent with a β -turn secondary structure as shown in Figure 3b.^{44,45} (Details may be found in the Supporting Information.)

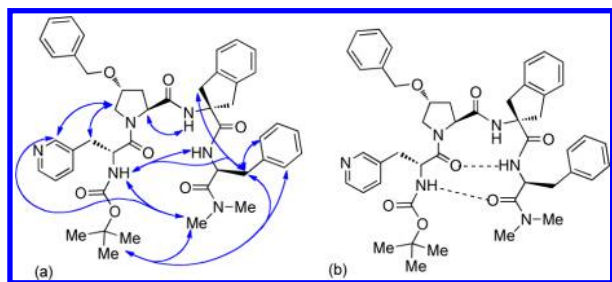


Figure 3. (a) NOE contacts for peptide catalyst **4i**. (b) β -Turn secondary structure consistent with the observed NOE data.

Even with knowledge about the three-dimensional structure of the catalyst, the exact origin of stereoinduction is not fully understood. A detailed confirmation of a catalyst–substrate adduct (e.g., of type **Ia** or **Ib**, Scheme 3) was not possible. However, when probed by ^1H NMR (see the Supporting Information for full details), a comixture of catalyst and substrate reveals some differences (the stacked spectra are shown in Figure 4). Notably, when Figure 4c (allenoate **1g**) is compared to Figure 4b (**4i** + allenoate **1g**), a significant downfield shift of the allenic amide NH resonance (Figure 4♦), by approximately 0.2 ppm is observed. However, for Figure 4c (allenoate **1g**) and 4d (**1g** + pyridine) no shifting of **1g** peaks is detected under these conditions. This observation, which is consistent with a hydrogen bond between peptide catalyst and substrate, may portend a multifunctional interaction between catalyst and substrate in the transition state. As noted above (eq 6), in the absence of the NH in the allenic ester, the observed selectivity in the couplings is greatly eroded. A putative interaction of this type could serve to activate the allene, consistent with the heightened reactivity observed with pyridyl peptide catalyst compared to pyridine (vide supra, eqs 7 and 8).

It may also be of significance that, as shown in Figure 4c, only a slight perturbation (0.03 ppm) is observed for the diagnostic^{44,45} downfield NH_{Phe} peak (Figure 4★), which is

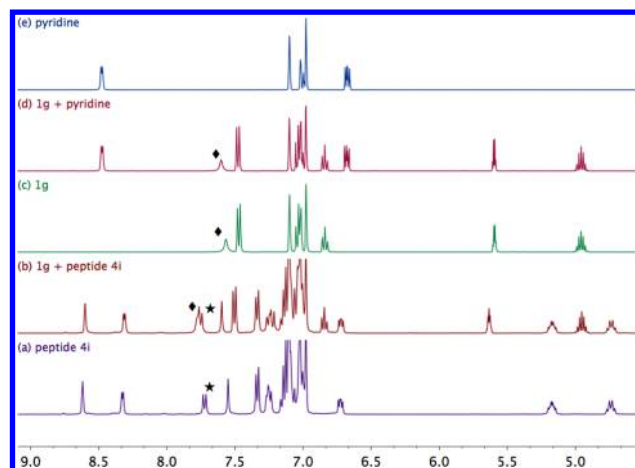


Figure 4. Catalyst and allenoate ^1H NMR spectra in toluene- d_8 : (a) peptide **4i**; (b) allenoate **1g** and peptide **4i**; (c) allenoate **1g**; (d) allenoate **1g** and pyridine; (e) pyridine. (♦: allenoate **1g** NH peak, ★: peptide **4i** NH_{Phe} peak).

invoked in the intramolecular H-bonding array of the β -hairpin. Based on this result, it is conceivable that the catalyst β -turn structure and catalyst–substrate H-bonding interactions may be maintained simultaneously in the transition state leading to significant levels of selectivity.

With these experimental observations in hand, we have considered a working model that is consistent with the significant selectivity we have observed. Figure 5 shows an

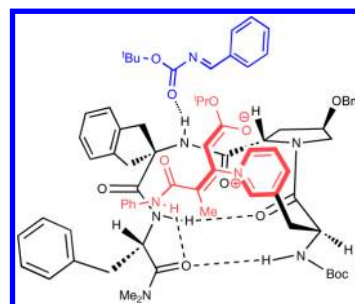


Figure 5. Speculative model for the addition reaction leading to **3j**.

allenoate–catalyst adduct **I** (Scheme 3) with the peptide maintaining its β -turn secondary structure (Figure 3b) and the allenic NH contacting the catalyst Phe-carbonyl oxygen via H-bonding. (We reiterate that in the absence of this NH in the allenic ester, we observe low selectivity; eq 6.) Carbon–carbon bond formation with the imine might then occur with simultaneous association of the imine electrophile through an additional H-bond, with an available NH of the catalyst (e.g., Aic-NH). This highly ordered, multivalent assembly⁴⁶ would place the imine in close proximity to the α -carbon of the zwitterion, facilitating bond formation. These notions are consistent with the heightened reactivity observed with pyridyl peptide catalyst compared to pyridine as catalyst (eqs 7 and 8). This model also accounts for the observation that peptide catalyst **4a** (Table 1), with the epimeric Phe residue at the *i* + 3 position, exhibits lower selectivity (Table 1, entries 1 and 2), since the allenic anilide and the Phe side chain would compete for the same space in this scenario. Yet it is appropriate to state that these models remain speculative in the absence of more definitive studies.

CONCLUSION

In conclusion, we have developed a highly diastereo- and enantioselective addition of allenic esters to *N*-acylimines. Our results include the study of allenates containing unsymmetrical carboxylic acid functional groups (ester versus amide) at the allene termini in these additions for the first time, revealing mechanistic consequences. These chiral tetrasubstituted allenes could serve as chiral building blocks for applications in synthetic chemistry. In addition, the differential substitution pattern in these products allows for orthogonal functionalization. Our data supports nucleophilic catalysis as the mode of reaction, and while our mechanistic data is still preliminary we have proposed a hypothetical mechanistic model that is consistent with the observed reactivity and selectivity.

ASSOCIATED CONTENT

Supporting Information

Full experimental details, characterization, and X-ray crystallographic data. This material is available free of charge via the Internet at <http://pubs.acs.org>.

AUTHOR INFORMATION

Corresponding Author

scott.miller@yale.edu

Notes

The authors declare no competing financial interest.

ACKNOWLEDGMENTS

We are grateful to the National Science Foundation (CHE-0848224) for financial support and to Louise Guard for X-ray crystallography. Partial support from the Israel–US Binational Science Foundation is also acknowledged. All experiments involving allenic substrate **1a** were conducted by Megan Brennan and Lindsey B. Saunders.

REFERENCES

- (1) Hoffmann-Röder, A.; Krause, N. *Angew. Chem., Int. Ed.* **2004**, *43*, 1196.
- (2) Krause, N.; Hoffmann-Röder, A. In *Modern Allene Chemistry*; Krause, N., Hoffmann-Röder, A., Eds.; Wiley-VCH: Weinheim, 2004; p 997.
- (3) Yu, S. C.; Ma, S. M. *Angew. Chem., Int. Ed.* **2012**, *51*, 3074.
- (4) Brummond, K. M.; Chen, H. In *Modern Allene Chemistry*; Krause, N., Hoffmann-Röder, A., Eds.; Wiley-VCH: Weinheim, 2004; p 1041.
- (5) Tejedor, D.; Mendez-Abt, G.; Cotos, L.; Garcia-Tellado, F. *Chem. Soc. Rev.* **2013**, *42*, 458.
- (6) Brasholz, M.; Reissig, H. U.; Zimmer, R. *Acc. Chem. Res.* **2009**, *42*, 45.
- (7) Aubert, C.; Fensterbank, L.; Garcia, P.; Malacria, M.; Simonneau, A. *Chem. Rev.* **2011**, *111*, 1954.
- (8) Bates, R. W.; Satcharoen, V. *Chem. Soc. Rev.* **2002**, *31*, 12.
- (9) Cowen, B. J.; Miller, S. J. *Chem. Soc. Rev.* **2009**, *38*, 3102.
- (10) Na, R. S.; Jing, C. F.; Xu, Q. H.; Jiang, H.; Wu, X.; Shi, J. Y.; Zhong, J. C.; Wang, M.; Benitez, D.; Tkatchouk, E.; Goddard, W. A.; Guo, H. C.; Kwon, O. Y. *J. Am. Chem. Soc.* **2011**, *133*, 13337.
- (11) Ohno, H.; Nagaoka, Y.; Tomioka, K. In *Modern Allene Chemistry*; Krause, N., Hoffmann-Röder, A., Eds.; Wiley-VCH: Weinheim, 2004; p 141.
- (12) Ogasawara, M. *Tetrahedron: Asymmetry* **2009**, *20*, 259.
- (13) Li, Z. J.; Boyarskikh, V.; Hansen, J. H.; Autschbach, J.; Musaev, D. G.; Davies, H. M. L. *J. Am. Chem. Soc.* **2012**, *134*, 15497.
- (14) Hayashi, T.; Tokunaga, N.; Inoue, K. *Org. Lett.* **2004**, *6*, 305.
- (15) Hammel, M.; Deska, J. *Synthesis* **2012**, *44*, 3789.
- (16) Pu, X. T.; Qi, X. B.; Ready, J. M. *J. Am. Chem. Soc.* **2009**, *131*, 10364.
- (17) Imbriglio, J. E.; Vasbinder, M. M.; Miller, S. J. *Org. Lett.* **2003**, *5*, 3741.
- (18) Aroyan, C. E.; Vasbinder, M. M.; Miller, S. J. *Org. Lett.* **2005**, *7*, 3849.
- (19) Vasbinder, M. M.; Imbriglio, J. E.; Miller, S. J. *Tetrahedron* **2006**, *62*, 11450.
- (20) Evans, C. A.; Miller, S. J. *J. Am. Chem. Soc.* **2003**, *125*, 12394.
- (21) Evans, C. A.; Cowen, B. J.; Miller, S. J. *Tetrahedron* **2005**, *61*, 6309.
- (22) Hashimoto, T.; Sakata, K.; Tamakuni, F.; Dutton, M. J.; Maruoka, K. *Nat. Chem.* **2013**, *5*, 240.
- (23) Cowen, B. J.; Saunders, L. B.; Miller, S. J. *J. Am. Chem. Soc.* **2009**, *131*, 6105.
- (24) Saunders, L. B. Doctoral Thesis, Yale University, 2012.
- (25) Jakobsche, C. E.; Peris, G.; Miller, S. J. *Angew. Chem., Int. Ed.* **2008**, *47*, 6707.
- (26) Vasbinder, M. M.; Jarvo, E. R.; Miller, S. J. *Angew. Chem., Int. Ed.* **2001**, *40*, 2824.
- (27) Price, K. E.; Broadwater, S. J.; Walker, B. J.; McQuade, D. T. *J. Org. Chem.* **2005**, *70*, 3980.
- (28) Price, K. E.; Broadwater, S. J.; Jung, H. M.; McQuade, D. T. *Org. Lett.* **2005**, *7*, 147.
- (29) Robiette, R.; Aggarwal, V. K.; Harvey, J. N. *J. Am. Chem. Soc.* **2007**, *129*, 15513.
- (30) Aggarwal, V. K.; Fulford, S. Y.; Lloyd-Jones, G. C. *Angew. Chem., Int. Ed.* **2005**, *44*, 1706.
- (31) Wenzel, A. G.; Jacobsen, E. N. *J. Am. Chem. Soc.* **2002**, *124*, 12964.
- (32) Raheem, I. T.; Jacobsen, E. N. *Adv. Synth. Catal.* **2005**, *347*, 1701.
- (33) Buskens, P.; Klankermayer, J.; Leitner, W. *J. Am. Chem. Soc.* **2005**, *127*, 16762.
- (34) Saunders, L. B.; Cowen, B. J.; Miller, S. J. *Org. Lett.* **2010**, *12*, 4800.
- (35) Hall, H. K.; Bates, R. B. *Tetrahedron Lett.* **2012**, *53*, 1830.
- (36) Brotzel, F.; Kempf, B.; Singer, T.; Zipse, H.; Mayr, H. *Chem.—Eur. J.* **2007**, *13*, 336.
- (37) Ammer, J.; Baidya, M.; Kobayashi, S.; Mayr, H. *J. Phys. Org. Chem.* **2010**, *23*, 1029.
- (38) Odiaka, T. I.; Kane-Maguire, L. A. P. *J. Chem. Soc., Dalton Trans.* **1981**, 1162.
- (39) Pearson, R. G.; Sobel, H. R.; Songstad, J. *J. Am. Chem. Soc.* **1968**, *90*, 319.
- (40) Bruckner, R. *Organic Mechanisms Reactions, Stereochemistry and Synthesis*; Springer Verlag: Berlin, 2010.
- (41) Wei, Y.; Sastry, G. N.; Zipse, H. *J. Am. Chem. Soc.* **2008**, *130*, 3473.
- (42) Denmark, S. E.; Beutner, G. L. *Angew. Chem., Int. Ed.* **2008**, *47*, 1560.
- (43) Anslyn, E. V.; Dougherty, D. A. *Modern Physical Organic Chemistry*; University Science: Sausalito, CA, 2006.
- (44) Haque, T. S.; Little, J. C.; Gellman, S. H. *J. Am. Chem. Soc.* **1996**, *118*, 6975.
- (45) Rose, G. D.; Gierasch, L. M.; Smith, J. A. *Adv. Protein Chem.* **1985**, *37*, 1.
- (46) Knowles, R. R.; Jacobsen, E. N. *Proc. Natl. Acad. Sci. U.S.A.* **2010**, *107*, 20678.